American Mineralogist, Volume 78, pages 1088–1095, 1993

Taikanite, $BaSr_2Mn_2^{3+}O_2[Si_4O_{12}]$, from the Wessels mine, South Africa: A chain silicate related to synthetic $Ca_3Mn_2^{3+}O_2[Si_4O_{12}]$

Thomas Armbruster
Laboratorium für chemische und mineralogische Kristallographie, Universität Bern, Freiestrasse 3, CH-3012 Bern, Switzerland
Roland Oberhänsli
Institut für Geowissenschaften, Universität Mainz, Saarstraße 21, D-6500 Mainz, Germany
Martin Kunz
Institute for Materials Research, McMaster University, Hamilton, Ontario L8S 4M1, Canada

Abstract

The chemical formula of taikanite from the Wessels mine, Kalahari, South Africa, has been revised to $BaSr_2Mn_2^{3+}O_2[Si_4O_{12}]$ and the crystal structure [space group $C2$, a = 14.600(2), b = 7.759(4), c = 5.142(1) Å, β = 93.25(2)°, Z = 2] has been determined and refined to R = 8% for 800 reflections with Mo$K\alpha$ X-radiation. An optically homogeneous crystal was separated from a conventional petrographic thin section (0.025 mm thick) with a microdrilling device mounted on a polarizing microscope. The composite sample used for structure determination consisted of upper and lower glass slides covering the thin crystal plate.

The structure is characterized by *vierer* single chains $[Si_4O_{12}]$ parallel to [010], which link edge-sharing zigzag chains of MnO_6 octahedra running parallel to [001]. Open channels in the structure are plugged by eightfold-coordinated Ba and Sr. The structure is related to that of synthetic $Ca_3Mn_2^{3+}O_2[Si_4O_{12}]$ [space group $I2/c$, a = 14.263(28), b = 7.620(13), c = 10.025(4) Å, β = 93.27(5)°, Z = 4], which has the *vierer* single chain $[Si_4O_{12}]$ in common. In the synthetic compound, $Mn^{3+}O_6$ octahedra form cis-trans-cis edge-sharing chains with a translation of 10.0 Å, whereas in taikanite the translation is only 5.1 Å, formed by cis-cis edge-sharing octahedra. The Mn2 octahedron in taikanite has four short and two long Mn^{3+}-O distances (elongated pseudotetragonal). The Mn1 octahedron has four intermediate and two short Mn^{3+}-O bonds (compressed pseudotetragonal). Both octahedral distortions are in agreement with bond valence requirements dictated by the structural topology and by the Jahn-Teller theorem.

Introduction

In the course of a thin section study of Mn^{3+} minerals from the Wessels mine, Kalahari, South Africa (Von Bezing et al., 1991; Dixon, 1989), we noticed a strongly pleochroic mineral (green, blue), which occurred in a fine-grained matrix of serandite-pectolite with minor sugilite and a new amphibole containing K, Na, Li, and Mn^{3+} (Armbruster et al., 1993). The dark green mineral forms grains up to 1 mm in diameter composed of twinned individuals. Preliminary electron microprobe analyses indicated a strontium barium manganese silicate with strong similarities to taikanite $Sr_3BaMn_2Si_4O_{14}$. Taikanite, associated with braunite and manganese amphibole in hydrothermal Mn ores, was described by Kalinin et al. (1985) as a new mineral from the Taikan Mountains in the far east of the former USSR.

The aim of the present study is a description of the taikanite structure accompanied with a discussion of $^{[6]}Mn^{3+}$ Jahn-Teller distortions in related minerals and synthetic compounds.

Sample description and preparation

The sample containing taikanite came from a sugilite-cemented breccia of hausmannite and braunite collected at the Wessels mine, Kalahari, South Africa. These sugilite breccias occur in the middle of the ore body (Dixon, 1985). Pink veinlets of serandite-pectolite, sugilite, a new amphibole containing K, Na, Li, and Mn^{3+} (kornite) (Armbruster et al., 1993), and a rare $SrMn_2[Si_2O_7](OH)_2 \cdot H_2O$ mineral of the lawsonite structure type (Armbruster et al., 1992) formed along the contacts of the breccia fragments (Fig. 1). The compositions and optical properties of the serandite-pectolite crystals vary within the veinlets. X_{Ca} ranges from 0.183 to 0.485, and the crystals change from pink to colorless. In addition, thin sections of the veinlets show occasional dark red to orange-yellow crystals. These rare crystals are extremely Pb rich, and preliminary microprobe analyses yielded the composition $(Pb_{1.7}Ba_{0.16})_{\Sigma=1.86}Mn_{2.02}^{3+}O_2[Si_2O_7]$ and are probably the disilicate kentrolite $PbMn_2O_2[Si_2O_7]$ (Moore et al., 1991),

0003–004X/93/0910–1088$02.00

which has already been described from the Wessels mine (Von Bezing et al., 1991).

The sugilite breccia contains sugilite and strongly pleochroic acmite (aegirine) with a blue-green tint (Table 1 and Dixon, 1989). The pink veinlets are zoned, showing a rim of aegirine and the amphibole containing K, Na, Li, and Mn^{3+}. The center of the veinlets are dominated by a zone of comblike serandite-pectolite. Within this serandite-pectolite zone, fibers of kornite and ideomorphic sugilite have grown obliquely to the veinlets. Aggregates of taikanite occur in this serandite-pectolite felt. Taikanite is strongly pleochroic (blue-green, turquoise, dark marine blue) and has a preferred orientation oblique to the vein walls. Most taikanite is prismatic but some samples form fine intergrowths with serandite-pectolite.

In sections thicker than a conventional petrographic thin section (>0.025 mm), taikanite from the Wessels mine appears nontransparent. Thus the twinning and intergrowth, combined with the dark color, prevented separation of single crystals from a hand specimen. We used the microdrilling device of Medenbach (1986) to obtain an untwinned crystal of this striking mineral for structure analysis. An optically homogeneous (untwinned) cylinder, 0.4 mm in diameter, was drilled out of the petrographic thin section (0.025 mm thick) during simultaneous observation under the polarizing microscope. The cylinder was composed of a sandwich structure of 0.2-mm glass on the bottom, 0.025-mm crystal, and 0.05-mm cover glass slide. Previous experiments to separate the crystal plate from the adhering glass failed because the test crystal cracked into tiny fragments. In addition, a regular disk mounted with its shortest dimension par-

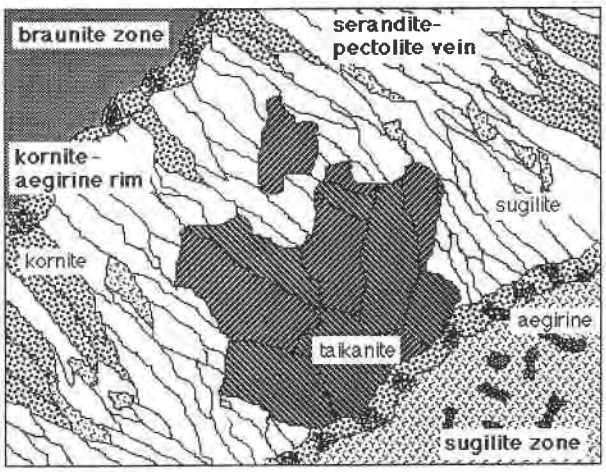

Fig. 1. Sketch of a taikanite-bearing thin section (ca. 0.6 × 0.5 cm) from the Wessels mine, Kalahari, South Africa.

Table 1. Chemical composition of taikanite and associated minerals

	Taikan*	Wessels mine						
	Taik.	Taik.	Taik.	Taik.	Korn.	Sugi.	Acmi.	Sera.
SiO_2	27.17	32.50	32.31	32.41	56.75	69.39	52.12	52.01
Al_2O_3		0.09	0.07	0.08	0.36	2.35	0.33	0.02
Fe_2O_3		0.00	0.03	0.00	9.39	11.47	23.80	0.03
Mn_2O_3		20.59	21.22	21.37	9.93	1.65	9.60	
MnO	19.42							31.11
MgO	0.14	0.00	0.00	0.00	9.15	0.00	0.33	0.08
CaO	0.46	0.29	0.29	0.27	0.21	0.04	0.45	6.97
SrO	33.78	25.40	25.18	24.98	0.00	0.00	0.00	0.00
BaO	18.43	18.90	18.44	18.48	0.07	0.00	0.05	0.00
PbO		2.10	1.41	1.45	0.09	0.00	0.01	0.12
Li_2O**					1.96	4.40		
Na_2O	0.18	0.06	0.06	0.07	7.67	6.20	12.75	7.00
K_2O		0.01	0.03	0.02	3.83	4.35	0.34	0.00
Total	99.58	99.94	99.04	99.13	99.41	99.85	99.78	97.34
Si	3.86	4.07	4.06	4.06	8′	11.86	2.00	3′
Al		0.01	0.01	0.01	0.06	0.47	0.02	0.01
Fe^{3+}			0.00	0.00	1.00	1.48	0.69	0.00
Mn^{3+}		1.96	2.03	2 04	1.07	0.22	0.28	
Mn^{2+}	2.34							1.52
Mg	0.03	0.00	0.00	0.00	1.92	0.00	0.02	0.01
Ca	0.07	0.04	0.04	0.04	0.03	0.01	0.02	0.43
Sr	2.78	1.84	1.83	1.81	0.00	0.00	0.00	0.00
Ba	1.03	0.93	0.91	0.91	0.00	0.00	0.00	0.00
Pb		0.07	0.05	0.05	0.00	0.00	0.00	0.00
Li	0.05				1.11	3.03		
Na		0.02	0.02	0.02	2.10	2.06	0.95	0.78
K		0.00	0.01	0.00	0.69	0.95	0.02	0.00
O	14′	14′	14′	14′		30′	6′	

Note: korn. = kornite (amphibole containing K, Na, Li, and Mn^{3+}); sugi. = sugilite; acmi. = acmite; sera. = serandite. Formulas were normalized to the element with a prime. Each Wessels mine taikanite analysis represents an average of 10, 15, and 13 points of three clusters within one serandite veinlet.

* Data from Kalinin et al. (1985).

** The Li_2O content of kornite and sugilite was taken from ion probe analyses (Armbruster et al., 1993). Ion probe analyses also indicate that serandite bears varying amounts of Li_2O.

Table 2. Calculated X-ray powder pattern for taikanite from the Wessels mine and observed powder pattern for taikanite from the Taikan Mountains

	Wessels mine (this work)		Taikan Mountains (Kalinin et al., 1985)	
hkl	*d* (Å)	I_{calc}	*d* (Å)	I_{obs}
200	7.29	13		
110	6.85	19	6.95	30
001	5.13	24	5.14	
11$\bar{1}$	4.16	7	4.18	10
201	4.09	2	4.18	
111	4.06	16	4.04	10
020	3.88	12	3.90	10
400	3.64	25	3.65	30
220	3.42	34	3.44	40
31$\bar{1}$	3.29	88	3.27	70
311	3.14	76	3.16	50
021	3.095	31	3.068	30
40$\bar{1}$	3.054	47		
401	2.895	31	2.912	100
22$\bar{1}$	2.885	100		
221	2.815	90	2.832	90
510	2.729	25	2.750	20
420	2.656	19	2.666	10
002	2.567	43	2.569	80
130	2.547	31	2.569	
600	2.429	17	2.441	10
421	2.320	35	2.335	10
40$\bar{2}$	2.157	16		
22$\bar{2}$	2.081	23		
620	2.059	11		
222	2.028	15		
710	2.011	12		
62$\bar{1}$	1.944	11		
040	1.940	11		
530	1.935	28		
51$\bar{2}$	1.921	12		
71$\bar{1}$	1.908	11		
711	1.839	12		
60$\bar{2}$	1.817	10		
132	1.799	17		
24$\bar{1}$	1.769	13		
241	1.753	12		
602	1.717	11		
82$\bar{1}$	1.594	14		
53$\bar{2}$	1.574	12		
223	1.547	19		
821	1.547	11		
223	1.515	13		

Note: powder intensities for the Wessels mine taikanite were calculated for Cu$K\alpha$ radiation and Debye-Scherrer geometry. Only intensities >10 and those indexed by Kalinin et al. (1985) are listed (program LAZYPULVERIX: Yvon et al., 1977). Kalinin et al. (1985) also reported additional reflections with low *d* values (<2.3 Å), which cannot unmistakenly be indexed; thus those reflections are not listed.

allel to the ϕ axis of a CAD4 single-crystal diffractometer causes much less anisotropy in X-ray absorption than an irregular fragment. Therefore, all structural data reported in this study were obtained from this unusual sandwich.

Electron microprobe analyses

Analyses of taikanite and associated minerals (Table 1) were performed on a Camebax electron microprobe at 15 kV and 10 nA, using natural and synthetic mineral standards (olivine: Si, Fe; pyrophanite: Mn; $SrSiO_3$: Sr; barite: Ba; anorthite: Ca, Al) and applying a PAP correction procedure. Three clusters of taikanite were investigated within one serandite-pectolite veinlet. The mineral is homogeneous within itself, within a cluster, and also among the analyzed clusters. Standard deviations for 13 analyses performed on a taikanite aggregate are below 0.65 wt% except for SiO_2, where the standard deviation is 1.14 wt%. The idealized formula for this taikanite is $BaSr_2Mn^{3+}_2O_2[Si_4O_{12}]$, with minor Ca and Pb substituting for Ba and Sr.

Identification and X-ray data measurement

All X-ray measurements on the glass-crystal-glass sandwich were performed at room temperature on a CAD4 single-crystal diffractometer with Mo$K\alpha$ X-radiation. Twenty-five automatically centered reflections could be indexed with a monoclinic *C*-centered lattice (space group *Cm*, *C*2, or *C*2/*m*): $a = 14.600(2)$, $b = 7.759(4)$, $c = 5.142(1)$ Å, $\beta = 93.25(2)°$, $V = 581.6(6)$ Å^3. The inorganic crystal structure data base (ICSD) of Bergerhoff et al. (1983) revealed no *C*-centered monoclinic silicate structure with a cell volume between 570 and 600 Å^3 and corresponding cell dimensions. Subsequently, the Mineral data base (Nickel and Nichols, 1991; Aleph Enterprises, 1991) was consulted for minerals with Ba, Sr, Mn, Si, and O, and the data bank proposed taikanite, $(Sr,Ba)_4Mn_2(Si_2O_7)_2$ (Kalinin et al., 1985), with similar cell dimensions: $a = 7.82$, $b = 14.60$, $c = 5.15$ Å, $\beta = 92.5°$ (space group *C*2/*m*). In the original description of taikanite (Kalinin et al., 1985) the idealized formula $Sr_3BaMn_2Si_4O_{14}$ or $(Sr,Ba)_5Mn_3Si_5O_{18}$ was given, Mn was assumed to be in the divalent state, and the calculated formula showed strong deviations from stoichiometry (Table 1). Thus the question arose whether $BaSr_2Mn^{3+}_2O_2[Si_4O_{12}]$ from the Wessels mine is identical to taikanite. The following arguments are in favor of the assumed identity: (1) strong similarity in cell dimensions, (2) space groups *C*2/*m*, *Cm*, and *C*2 show the same diffraction symmetry and can only be distinguished by a structure refinement, (3) similarity of the paragenesis, (4) similarity of optical appearance, (5) similarity in the qualitative chemical composition, (6) good agreement between measured X-ray powder intensities of taikanite from the Taikan Mountains and those calculated from the crystal structure (see below) of the Wessels mine sample (Table 2). It should be mentioned that two rather strong X-ray powder diffraction lines, at 3.054 ($I = 47$) and 2.895 Å ($I = 31$), were calculated for the Wessels mine taikanite but were not reported by Kalinin et al. (1985). We assume that the reflection at 3.068 Å by Kalinin et al. (1985) is actually a mixture of our calculated values at 3.095 and 3.054 Å. The 2.895-Å reflection was probably not resolved in the neighborhood of the strongest line, at 2.885 Å. The major discrepancy is found in the quantitative chemical composition. At this stage, we also noticed that the structure of taikanite was unknown, but the mineral was classified (Aleph Enterprises, 1991) as related to lamprophyllite (disilicate).

To solve the structure of taikanite, we obtained a standard X-ray intensity data set (Armbruster et al., 1992) up to $\theta = 30°$ in primitive triclinic symmetry. All significant

TABLE 3. Atomic coordinates and isotropic displacement parameters of taikanite

Atom	x	y	z	B (Å²)
Ba	0	0.22180	0	0.72(5)
Sr	0.2045(2)	−0.1035(5)	−0.0175(5)	0.52(5)
Mn1	0	−0.111(1)	½	0.45(9)
Mn2	0	−0.305(1)	0	0.5(1)
Si1	0.1309(6)	−0.428(1)	−0.538(2)	0.5(1)
Si2	−0.1736(6)	0.194(1)	0.487(2)	0.5(1)
O1	−0.097(2)	−0.277(4)	−0.665(4)	1.0(3)
O2	−0.164(2)	0.399(4)	−0.631(4)	1.0(3)
O3	−0.096(2)	0.084(3)	0.366(5)	0.8(4)
O4	0.059(1)	−0.126(3)	0.186(4)	0.4(3)
O5	0.181(1)	0.191(3)	0.206(4)	0.6(3)
O6	0.062(2)	0.520(3)	0.220(5)	0.9(4)
O7	−0.272(2)	0.139(3)	−0.667(4)	0.4(3)

reflections were in agreement with *C* centering. Data reduction was done with the SDP program system (Enraf-Nonius, 1983). Absorption was partly corrected by ψ scans. Transmission factors ranged between 36 and 99%. Averaging of symmetry-equivalent reflections yielded only an agreement factor (on intensity) of 10%, indicating that we were unable to correct completely for the severe anisotropy of absorption. If one compares the linear absorption coefficients (Mo$K\alpha$ X-radiation) for glass (ca. 6 cm^{-1}) vs. taikanite (ca. 182 cm^{-1}) and accounts for the shape of the sandwich sample, then it becomes evident that the major contribution of the anisotropic absorption comes from the disk shape of the taikanite crystal and not from the surrounding glass. The main influence of the glass is an increase of the background to peak ratio. A more sophisticated absorption model was not applied because the agreement factor of symmetry-equivalent reflections (10%) already indicated that we would be able to resolve the structural topology of taikanite with these data. The structure was solved by direct methods with the program SHELXS (Sheldrick, 1986) in space group *C*2 after no reasonable structure could be obtained in *C*2/*m*, as proposed by Kalinin et al. (1985). The refinement based on 800 unique reflections was carried out with the program SHELX76 (Sheldrick, 1976) using neutral-atom scattering factors and both real and imaginary dispersion corrections. The final *R* value converged at 8% with isotropic displacement parameters.

RESULTS

Refined atomic coordinates and isotropic displacement parameters are summarized in Table 3, observed and calculated structure factors are given in Table 4,[1] and interatomic distances and angles are listed in Table 5. The taikanite structure is composed of zigzag chains of edge-sharing $Mn^{3+}O_6$ octahedra running parallel to [001] (Fig. 2), in which the shared edges within each octahedron are connected in a semiadjacent way. We will refer to this

[1] A copy of Table 4 may be obtained by ordering Document AM-93-534 from the Business Office, Mineralogical Society of America, 1130 Seventeenth Street NW, Suite 330, Washington, DC 20036. Please remit $5.00 in advance for the microfiche.

TABLE 5. Interatomic distances (Å) and angles (°) for taikanite

Ba-O3	2.63 (2×)	Mn1-O1	2.06 (2×)	O3-Mn1-O4	95
-O4	2.98 (2×)	-O3	2.15 (2×)	O3-Mn1-O1	84
-O5	2.81 (2×)	-O4	1.88 (2×)	O3-Mn1-O3	90
-O6	2.71 (2×)			O3-Mn1-O4	90
				O4-Mn1-O1	86
Sr-O1	2.58			O4-Mn1-O1	89
-O2	2.69				
-O3	2.75	Mn2-O1	2.30 (2×)		
-O4	2.43	-O4	1.87 (2×)	O4-Mn2-O1	80
-O5	2.54	-O6	1.96 (2×)	O4-Mn2-O6	92
-O5	2.59			O4-Mn2-O1	92
-O7	2.70			O4-Mn2-O4	84
-O7	2.71			O1-Mn2-O6	85
				O1-Mn2-O4	92
Si1-O1	1.66	O1-Si1-O2	109		
-O2	1.66	O1-Si1-O6	118		
-O6	1.60	O1-Si1-O7	109		
-O7	1.68	O2-Si1-O6	111		
		O2-Si1-O7	103		
		O6-Si1-O7	106		
Si2-O2	1.71	O2-Si2-O3	107	Si1-O2-Si2	127
-O3	1.58	O2-Si2-O7	99	Si1-O7-Si2	128
-O5	1.59	O2-Si2-O5	112		
-O7	1.66	O3-Si2-O7	107		
		O3-Si2-O5	118		
		O7-Si2-O5	111		

Note: estimated standard deviations of distances are <0.03 Å; estimated standard deviations of angles are ca. 1°.

type of arrangement as a cis-cis arrangement (Fig. 3 left). These octahedral chains are interwoven with undulating *vierer* single chains [Si_4O_{12}] running parallel to [010] (Fig. 2). Si1 tetrahedra share two corners with MnO_6 tetrahedra. Two types of channels occur along [001]. The larger channels are occupied by eightfold-coordinated Ba (average Ba-O distance = 2.78 Å), and the smaller ones by eightfold-coordinated Sr (average Sr-O distance = 2.62 Å). The $Mn^{3+}O_6$ octahedra are strongly distorted. Mn2 has four short and two long Mn-O distances, leading to an elongated octahedron (2 × 1.87, 2 × 1.96, and 2 × 2.30 Å). Mn1 displays a compressed octahedron with 2 × 1.88, 2 × 2.06, and 2 × 2.15 Å.

DISCUSSION

Liebau's (1985) systematic analysis of silicates reveals that synthetic CMS-XI, $Ca_3Mn_2^{3+}O_2[Si_4O_{12}]$ (Anastasiou and Langer, 1977), has a very similar structure with *vierer* single chains (Moore and Araki, 1979). The major difference between CMS-XI and taikanite occurs parallel to [001]. CMS-XI is composed of undulating cis-trans-cis octahedral edge-sharing chains with a 10-Å translation period (Fig. 3). In taikanite the sinusoidal undulating chains have a cis-cis connectivity with a 5.1-Å translation period. A consequence of this difference in edge-sharing is an expansion of the size and shape of alkaline earth ion positions. Thus Ba and Sr in taikanite have fairly regular eightfold coordination [$d(\text{Ba-O})_{max} - d(\text{Ba-O})_{min} = 0.3$ Å; $d(\text{Sr-O})_{max} - d(\text{Sr-O})_{min} = 0.3$ Å], whereas the corresponding coordination of Ca1 and Ca2 in CMS-XI is irregular eightfold [$d(\text{Ca1-O})_{max} - d(\text{Ca1-O})_{min} = 0.83$ Å; $d(\text{Ca2-O})_{max} - d(\text{Ca2-O})_{min} = 0.54$ Å], respectively. The substitution Ba + 2Sr for 3Ca leads to an increase of all

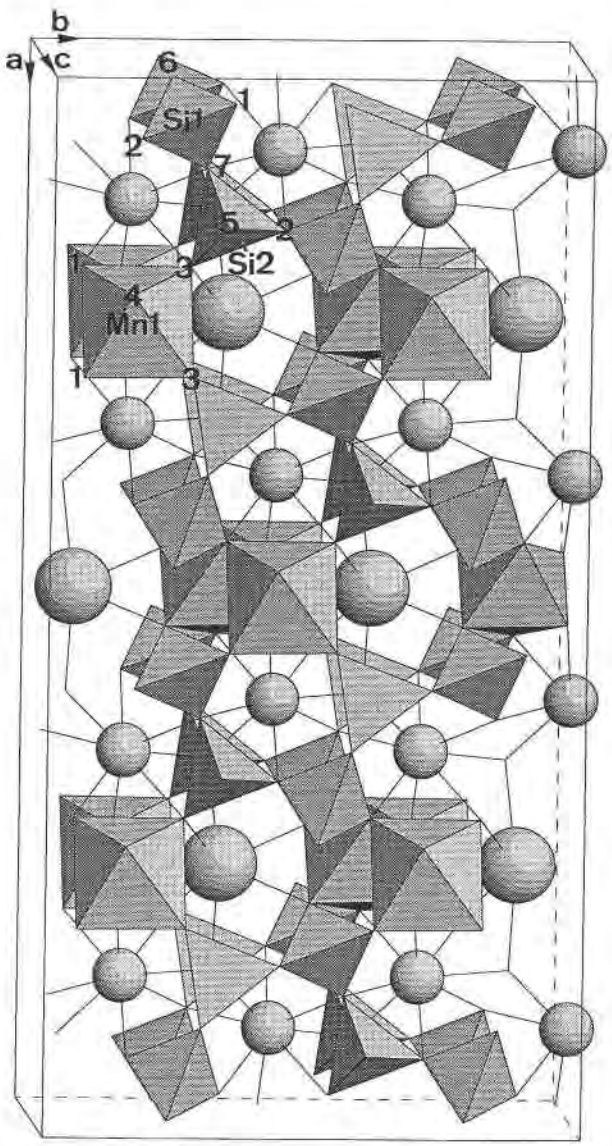

Fig. 2. Polyhedral model of the taikanite structure displaying tetrahedral *vierer* single chains running parallel to **b**. Large spheres are Ba, smaller spheres are Sr.

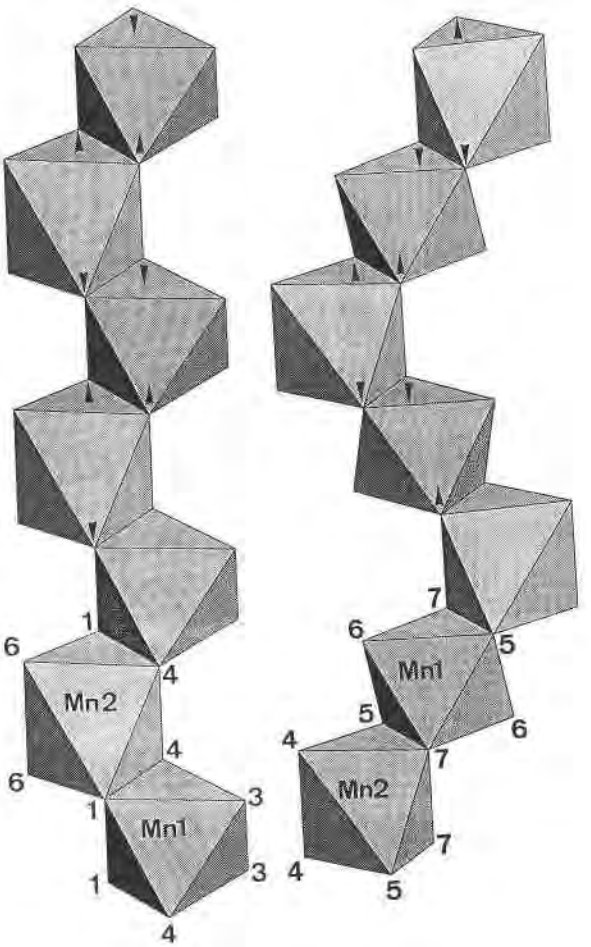

Fig. 3. Polyhedral models of the edge-sharing $^{[6]}Mn^{3+}$ chains running parallel to **c** in taikanite and in CMS-XI (Moore and Araki, 1979). **(Left)** the cis-cis connectivity of taikanite and **(right)** the cis-trans-cis connectivity of CMS-XI. Arrows indicate the orientation of octahedral compression or elongation.

three cell dimensions by 2–3%. In both structures the tetrahedral zigzag chains lie in the (001) plane. In taikanite, the larger ionic radius of Ba and Sr vs. Ca leads to a slight stretching of the tetrahedral chains: Si1-O1-Si2 (125.3°) and Si1-O2-Si2 (126.3°) in CMS-XI, corresponding to Si1-O2-Si2 (127°) and Si1-O7-Si2 (128°) in taikanite, respectively.

The application of the bond valence approach of Brown and Altermatt (1985), using the constants of Brese and O'Keefe (1991), shows that the Ca1 of CMS-XI (Moore and Araki, 1979) is strongly and the Ca2 slightly underbonded, with bond valence sums = 1.78 and 1.90 valence units (vu), respectively (Table 6). In contrast, Ba and Sr in taikanite are considerably overbonded, yielding bond valence sums of 2.24 and 2.15 vu, respectively. This is mainly related to the rigidity of the tetrahedral-octahedral framework, which cannot readily adopt to the ionic size of the alkaline earth ions. Taking into account these deviations of the bond valence sums from their ideal values, as well as the structural features, we propose that the structural differences between these two compounds are a result of both the chemical substitution (Ba + 2Sr for 3Ca) and different stability ranges of the two structures: CMS-XI is stable only at high pressure, >13 kbar, and 800 °C (Anastasiou and Langer, 1977). The taikanite-bearing, sugilite-rich rock was formed by a hydrothermal event at an estimated pressure of approximately 1 kbar and a maximum of 450 °C (Dixon, 1989). Under high-pressure conditions, the structure of CMS-XI would be compressed, and the Ca-O distances would be shortened, leading to increased and more ideal bond-valence sums. If, on the other hand, the structure of taikanite would be further compressed, the overbonding of Ba and Sr would

Table 6. Calculated and observed bond valences for taikanite and CMS-XI

	O1	O2	O3	O4	O5	O6	O7	Total
				Taikanite				
Ba_{calc}			0.172 (× 2)	0.331 (× 2)	0.217 (× 2)	0.28 (× 2)		2.0
Ba_{obs}			0.395 (× 2)	0.155 (× 2)	0.255 (× 2)	0.315 (× 2)		2.24
Sr_{calc}	0.225	0.147	0.290	0.449	0.335 (× 2)		0.110 (× 2)	2.0
Sr_{obs}	0.287	0.22	0.186	0.44	0.328		0.207	2.15
					0.278		0.203	
$Mn1_{calc}$	0.403 (× 2)		0.469 (× 2)	0.628 (× 2)				3.0
$Mn1_{obs}$	0.449 (× 2)		0.356 (× 2)	0.736 (× 2)				3.08
$Mn2_{calc}$	0.367 (× 2)			0.592 (× 2)		0.541 (× 2)		3.0
$Mn2_{obs}$	0.236 (× 2)			0.756 (× 2)		0.591 (× 2)		3.17
$Si1_{calc}$	1.005	0.927				1.178	0.89	4.0
$Si1_{obs}$	0.941	0.957				1.121	0.926	3.95
$Si2_{calc}$		0.926	1.069		1.114		0.89	4.0
$Si2_{obs}$		0.83	1.196		1.137		0.961	4.12
O_{calc}	2.0	2.0	2.0	2.0	2.0	2.0	2.0	
O_{obs}	1.91	2.01	2.13	2.09	2.00	2.03	2.30	
				CMS-XI				
$Ca1_{calc}$	0.015 (× 2)		0.205 (× 2)	0.283 (× 2)		0.171 (× 2)	0.326 (× 2)	2.0
$Ca1_{obs}$	0.027 (× 2)		0.106 (× 2)	0.341 (× 2)		0.375 (× 2)	0.04 (× 2)	1.78
$Ca2_{calc}$	0.142	0.110 (× 2)	0.332 (× 2)		0.222	0.298	0.453	2.0
$Ca2_{obs}$	0.165	0.123	0.36		0.248	0.225	408	1.90
		0.094	0.274					
$Mn1_{calc}$					0.398 (× 2)	0.474 (× 2)	0.629 (× 2)	3.0
$Mn1_{obs}$					0.435 (× 2)	0.341 (× 2)	0.774 (× 2)	3.10
$Mn2_{calc}$				0.548 (× 2)	0.360 (× 2)		0.592 (× 2)	3.0
$Mn2_{obs}$				0.574 (× 2)	0.235 (× 2)		0.727 (× 2)	3.07
$Si1_{calc}$	0.941	0.909	1.131		1.02			4.0
$Si1_{obs}$	0.980	0.937	1.150		1.092			4.16
$Si2_{calc}$	0.902	0.871		1.170		1.058		4.0
$Si2_{obs}$	0.927	0.940		1.098		1.089		4.05
O_{calc}	2.0	2.0	2.0	2.0	2.0	2.0	2.0	
O_{obs}	2.10	2.09	1.89	2.01	2.01	2.03	1.95	

Note: network equations from Brown (1992a, 1992b).

increase, and the structure would become unstable. The change from the cis-cis octahedral chain in taikanite to a cis-trans-cis chain in CMS-XI may be explained by the higher compressibility of the cis-trans-cis chain compared with the cis-cis arrangement. This gives the *c* axis more flexibility to react to increased pressure, allowing a shortening of the *c* axis in CMS-XI (c = 10.025 Å) compared with taikanite (2 × 5.148 Å = 10.296 Å).

The bond lengths of the two structures were modeled using the bond-valence concept of Brown (1992a, 1992b). In this method the infinite three-dimensional geometry of the structure is first projected into a two-dimensional finite graph. Applying the two network equations (bond-valence sum rule, equal valence rule) on this bond graph, one is able to predict ideal bond lengths for a given bonding topology. These calculations were done using the program Strumo (Brown, 1989). It has to be kept in mind that, as a result of the projection of the three-D structure onto a finite bond graph, any information on the geometry of the structure is lost. This implies that predictions emerging from the network equations represent ideal bond lengths, neglecting any possible internal strain caused by the particular geometry of a given structure. Therefore, bond lengths derived from the bond valence model do not necessarily fit into a three-D arrangement. Table 6 compares observed (structure refinement) and calculated (Brown, 1992a, 1992b) bond valences for both structures.

For Mn2 in taikanite and in CMS-XI, the network equations predict a bond-length arrangement leading to an elongated octahedron. Such a distortion can be fulfilled by high-spin Mn^{3+}, if, in addition to the three d electrons on the t_{2g} suborbitals, the remaining fourth electron populates the d_{z^2} lobe (e.g., Burns, 1970; Moore et al., 1991). This distortion is in agreement with the most frequent variety of the well-known Jahn-Teller effect for Mn^{3+} (Dunitz and Orgel, 1957).

In the Mn1 position in taikinite a bond length distribution of four medium and two short Mn^{3+}-O distances occurs rather than the expected pattern of four short and two long observed for Mn2. In addition, the two longest distances of the type Mn1-O3 are arranged in cis position, which is in contradiction to an axial $^{[6]}Mn^{3+}$ Jahn-Teller effect. The same bond length pattern is observed for the Mn1 position in CMS-XI. There are three possible explanations for the distorted Mn1 coordination:

1. A disordered Jahn-Teller distortion (e.g., Vedani, 1981) of the same type as the ordered distortion in Mn2 exists. In the assumed disorder, the long O-Mn^{3+}-O axis could either be along O3-Mn1-O1′ or O3′-Mn1-O1 (Fig. 3); thus the observed Mn1-O3 and Mn1-O1 bonds become averages of short and long Mn-O distances.

2. A different type of Jahn-Teller distortion, where the fourth electron populates the $d_{x^2-y^2}$ lobe instead of d_{z^2} leading to a compressed octahedron (Burns, 1970; Moore

et al., 1991) has taken place. Such a Jahn-Teller distortion is quite compatible with the theory but seems to be less frequent in Mn^{3+} and Cu^{2+} molecular structures (Dunitz and Orgel, 1957; Fackler and Avdeef, 1974).

3. A bond valence distortion overcomes the Jahn-Teller effect. In this case, the distortion caused by the topological connectivity and expressed by the calculated bond valences is assumed to remove the octahedral orbital degeneracy more efficiently than a possible Jahn-Teller effect, which even may act against the bond valence requirements.

Hypothesis 1 can easily be tested if anisotropic displacement parameters are available (Bürgi, 1989). In the case of a disordered Jahn-Teller distortion, increased difference displacement parameters, values of ΔU (by ca. 0.04 Å^2) should be observed along intermediate Mn-O distances. For taikanite this test cannot be applied, as only isotropic displacement parameters are available. However, as mentioned above, the Mn1 site of the CMS-XI structure (Moore and Araki, 1979) shows a bond-length distribution qualitatively identical to the corresponding taikanite position, and increases in ΔU must therefore be expected for the intermediate bonds. Calculations of ΔU along the critical bonds do not yield increased values. Therefore, the hypothesis of disorder in the orientation of the Jahn-Teller distortion can be rejected for CMS-XI. In taikanite isotropic displacement parameters (Table 3) of O1 and O3 (forming intermediate bonds) are about twice as large as that of O4 (forming the short bond); thus possible disorder cannot be completely excluded.

The axially compressed octahedra Mn1 in taikanite, Mn1 in CMS-XI, and Mn2 in kentrolite (Moore et al., 1991) agree with a Jahn-Teller distortion expected for occupied $d_{x^2-y^2}$ lobes. Furthermore, comparing the calculated bond-valence sum distribution with the observed geometry, one finds (Table 6) that the network equations predict for taikanite that the two Mn-O4 bonds will be the shortest, whereas the Mn-O3 and Mn-O1 bonds should be of equal intermediate length. A qualitatively corresponding pattern is found for CMS-XI. Both predicted patterns match the observed situation. Thus the structural topology of taikanite and CMS-XI is tailor-made for octahedral high-spin Mn^{3+}, which is able to form pseudotetragonally distorted octahedra with compressed and elongated forms.

This crystal chemical argument is supported by the geochemistry of the taikanite-bearing paragenesis at the Wessels mine: sugilite, kornite, and acmite (Armbruster et al., 1993) bear considerable amounts of Fe^{3+}, which was not found in significant concentrations in taikanite (Table 1). Fe^{3+} (d5 electron configuration) in oxides prefers the high-spin configuration, leading to less distorted octahedral geometry. This was also found in sugilite (Armbruster and Oberhänsli, 1988), where the Fe^{3+}-bearing octahedron possesses $\bar{3}$ symmetry, and in end-member acmite (Clarc et al., 1969), where Fe^{3+}-O distances vary between 1.94 and 2.11 Å.

In all three structures with chains of edge-sharing Mn^{3+} octahedra linked in a cis-trans-cis or cis-cis fashion. CMS-XI (Moore and Araki, 1979), kentrolite (Moore et al., 1991), and taikanite (this study), the unusually compressed pseudotetragonal, Jahn-Teller-deformed Mn^{3+} octahedra always have the compressed O-Mn^{3+}-O axes associated with the only O atom that is not bonded to Si. If we consider only the tetrahedral and octahedral ions in these structures (Si^{4+} and Mn^{3+}), the O atom not linked to Si appears to be strongly underbonded, which leads to a shortening of the corresponding Mn^{3+}-O bonds. Jahn-Teller-deformed octahedra of the pseudotetragonal compressed type (four intermediate and two short bonds) are less distorted with respect to their bond distances than the more frequent elongated type of octahedra (four short and two long bonds). Thus Mn^{3+} in the compressed octahedra may be substituted more easily by other cations, such as Al and Fe^{3+}, than Mn^{3+} in the elongated octahedra.

In CMS-XI and taikanite, compressed and elongated octahedra occur adjacent to each other, and the pseudotetragonal axes of the individual octahedra are parallel to each other (Fig. 3). However, this parallel arrangement cannot be considered a general rule, as kentrolite shows a different distribution.

Acknowledgments

We are indebted to Jürgen Abrecht (Bern) for providing hand specimens of Mn ores from the Wessels mine, Kalahari, South Africa. M.K. thanks the Swiss National Science Foundation for support during his stay at McMaster University, Hamilton, Ontario. An earlier version of this manuscript benefited from the constructive criticism of I.D. Brown and K. Langer.

References cited

Aleph Enterprises (1991) The Mineral Data Base, Livermore, California.

Anastasiou, P., and Langer, K. (1977) Synthesis and physical properties of piemontite $Ca_2Al_{3-p}Mn^{3+}_p(Si_2O_7/SiO_4/O/OH)$. Contributions to Mineralogy and Petrology, 60, 225–245.

Armbruster, Th., and Oberhänsli, R. (1988) Crystal chemistry of double-ring silicates: Structures of sugilite and brannockite. American Mineralogist, 73, 595–600.

Armbruster, Th., Oberhänsli, R., and Bermanec, V. (1992) Crystal structure of $SrMn_2[Si_2O_7](OH)_2 \cdot H_2O$, a new mineral of the lawsonite type. European Journal of Mineralogy, 4, 17–22.

Armbruster, Th., Oberhänsli, R., Bermanec, V., and Dixon, R. (1993) Hennomartinite and kornite, two new Mn^{3+} rich silicates from the Wessels Mine, Kalahari, South Africa. Schweizerische mineralogische und petrographische Mitteilungen, in press.

Bergerhoff, G., Hundt, R., Sievers, R., and Brown, I.D. (1983) The inorganic crystal structure database. Journal of Chemical Information and Computer Sciences, 23, 66–69.

Brese, N.E., and O'Keefe, M. (1991) Bond-valence parameters for solids. Acta Crystallographica, B47, 192–197.

Brown, I.D. (1989) Using chemical bonds to analyze data retrieved from the Inorganic Crystal Structure Database. Journal of Chemical Information and Computer Sciences, 29, 266–271.

——— (1992a) Modelling the structures of La_2NiO_4. Zeitschrift für Kristallographie, 199, 255–272.

——— (1992b) Chemical and steric constraints in inorganic salts. Acta Crystallographica, B48, 553–572.

Brown, I.D., and Altermatt, D. (1985) Bond valence parameters obtained from a systematic analysis of the Inorganic Crystal Structure Database. Acta Crystallographica, B41, 244–247.

Bürgi, H.B. (1989) Interpretation of atomic displacement parameters: In-

tramolecular translational oscillation and rigid-body motion. Acta Crystallographica, B45, 383–390.

Burns, R.G. (1970) Mineralogical applications of crystal field theory, p. 4–27. Cambridge University Press, New York.

Clarc, J.R., Appleman, E.E., and Papike, J.J. (1969) Crystal chemical characterization of clinopyroxenes based on eight new structure refinements. Mineralogical Society of America Special Paper, 2, 31–50.

Dixon, R.D. (1985) Sugilite and associated minerals from Wessels Mine, Kalahari manganese field. Transactions of the Geological Society of South Africa, 88, 11–17.

——— (1989) Sugilite and associated metamorphic silicate minerals from Wessels Mine Kalahari manganese field. Bulletin of the Geological Survey of South Africa, 93, 1–47.

Dunitz, J.D., and Orgel, L.E. (1957) Electronic properties of transition metal oxides I. Journal of Physical Chemistry of Solids, 3, 20–29.

Enraf-Nonius (1983) Structure determination package (SDP). Enraf-Nonius, Delft, The Netherlands.

Fackler, J.P., and Avdeef, A. (1974) Crystal and molecular structure of tris(2,4-pentanedionato)manganese(III), $Mn(O_2C_5H_7)_3$, a distorted complex as predicted by Jahn-Teller arguments. Inorganic Chemistry, 13, 1864–1875.

Kalinin, V.V., Dauletkulov, A.B., Gorshkov, A.I., and Troneva, N.V. (1985) Taikanite: A new silicate of strontium, barium, and manganese. Zapiski Vsesoyuznogo Mineralogicheskogo Obshchestva, 114, 635–641 (in Russian) (not seen; extracted from American Mineralogist, 72, 226, 1987).

Liebau, F. (1985) Structural chemistry of silicates: Structure, bonding, and classification, p. 103. Springer-Verlag, Berlin.

Medenbach, O. (1986) Ein modifiziertes Kristallbohrgerät nach Verschure (1978) zur Isolierung kleiner Einkristalle aus Dünnschliffen. Fortschritte der Mineralogie, Beiheft 64, 113.

Moore, P.B., and Araki, T. (1979) Crystal structure of synthetic $Ca_3Mn_2^{3+}O_2[Si_4O_{12}]$. Zeitschrift für Kristallographie, 150, 287–297.

Moore, P.B., Sen Gupta, P.K., Shen, J., and Schlemper, E.O. (1991) The kentrolite-melanotektite series, $4Pb_2(Mn,Fe)_2^{3+}O_2[Si_2O_7]$: Chemical crystallographic relations, lone-pair splitting, and cation relation to $8URe_2$. American Mineralogist, 76, 1389–1399.

Nickel, E.H., and Nichols, M.C. (1991) Mineral reference manual, 250 p. Van Nostrand Reinhold, New York.

Sheldrick, G.M. (1976) SHELX-76: Program for crystal structure determination. University of Cambridge, Cambridge, England.

——— (1986) SHELXS-86/Fortran-77: Program for the solution of crystal structures from diffraction data. Institut für anorganische Chemie der Universität Göttingen, Germany.

Vedani, A. (1981) Statische und dynamische Jahn-Teller-Verzerrungen in Mangan(III)- und Kupfer(II)-Verbindungen, 150 p. Inaugural-Dissertation der Universität Zürich, Zürich, Switzerland.

Von Bezing, K.L., Dixon, R.D., Pohl, D., and Cavallo, G. (1991) The Kalahari manganese field: An update. Mineralogical Record, 22, 279–297.

Yvon, K., Jeitschko, W., and Parthe, E. (1977) LAZYPULVERIX, a computer program, for calculating X-ray and neutron powder patterns. Applied Crystallography, 10, 73–74.

Manuscript received December 15, 1992
Manuscript accepted April 25, 1993